Metals **2015**, *5*, 1136-1147; doi:10.3390/met5031136

OPEN ACCESS

metals

ISSN 2075-4701

www.mdpi.com/journal/metals/

Article

Green Nanocomposites from Renewable Plant Oils and Polyhedral Oligomeric Silsesquioxanes

Takashi Tsujimoto [1,*], Hiroshi Uyama [1], Shiro Kobayashi [2], Hisao Oikawa [3] and Mikio Yamahiro [3]

[1] Department of Applied Chemistry, Graduate School of Engineering, Osaka University, Suita, Osaka 565-0871, Japan; E-Mail: uyama@chem.eng.osaka-u.ac.jp

[2] Center for Fiber and Textile Science, Kyoto Institute of Technology, Kyoto 606-8585, Japan; E-Mail: kobayash@kit.ac.jp

[3] Research Laboratory II, Ichihara Research Center, JNC Petrochemical Corporation, Goi-Kaigan, Ichihara, Chiba 290-8551, Japan; E-Mails: h.oikawa@jnc-corp.co.jp (H.O.); yamahiro@jnc-corp.co.jp (M.Y.)

***** Author to whom correspondence should be addressed; E-Mail: tsujimoto@chem.eng.osaka-u.ac.jp; Tel.: +81-6-6879-7365; Fax: +81-6-6879-7367.

Academic Editor: Nikolaos Michailidis

Received: 24 March 2015 / Accepted: 24 June 2015 / Published: 30 June 2015

Abstract: Green nanocomposites based on renewable plant oils and polyhedral oligomeric silsesquioxanes (POSS) have been developed. An acid-catalyzed curing of epoxidized plant oils with oxirane-containing POSS derivatives produced transparent nanocomposite coatings with high gloss surface, in which the organic and inorganic components were linked via covalent bonds. The hardness and mechanical strength were improved by the incorporation of the POSS unit into the organic polymer matrix. Nanostructural analyses of the nanocomposites showed the formation of homogeneous structures at the micrometer scale. On the other hand, such improvements of the coating and mechanical properties were not observed in the composite without covalent bonds between the plant oil-based polymer and POSS unit. The study demonstrates the correlation between the nanostructure of composites and macroscopic properties.

Keywords: polyhedral oligomeric silsesquioxane; renewable resource; epoxidized plant oil; hybrid material

1. Introduction

Recently, there has been an enormous interest in organic-inorganic nanocomposites as next generation materials because of their high potentials to realize novel properties and to tailor these properties. When the sizes of organic and inorganic components approach the nanometer scale, synergistic combination of their individual properties will provide new nanocomposite materials with improved properties [1–4].

Polyhedral oligomeric silsesquioxanes (POSSs) consist of inorganic framework made from a proportion of silicon and oxygen ($SiO_{1.5}$). Octahedral derivatives are the most representative ones of this family. POSSs have been extensively studied as a starting substrate to construct nanocomposites with precise control of nanoarchitecture and properties [5–11]. However, the procedure of blending POSS in a polymer matrix often meets severe problems with aggregation of POSS units, limiting the POSS amount introduced deteriorating the properties [12–14]. So far, a variety of functional POSS derivatives have been developed. Polymerizable POSS macromers, such as vinyl-functionalized POSS and oxirane-functionalized POSS, have been employed to copolymerize with organic monomers to afford a variety of polymer/POSS nanocomposites [15–27]. Polymerizable POSSs make a covalent attachment to a polymer matrix possible, and POSS units are well-dispersed in a polymer matrix. Lee and Lichtenhan used macromers of oxirane-functionalized POSS in reaction with diglycidylether of bisphenl-A in order to change the vitrification temperature [28]. Laine *et al*. synthesized two oxirane-functionalized POSSs and prepared POSS nanocomposites with diaminodiphenylmethane as a hardener [29]. Zheng *et al*. investigated the morphology and thermal properties of POSS containing epoxy hybrid [30]. In these cases, the nano-sized cage structures are incorporated into common plastics by copolymerization or grafting to improve their various properties such as thermal stability, oxidation resistance, oxygen permeability, low permittivity, and low refractive index. This may be because uniformly dispersed organic/inorganic components synergistically change bulk properties.

Worldwide potential demands for replacing petroleum-derived raw materials with renewable plant-based ones in production of polymeric materials are quite significant in the social and environmental viewpoints [31]. Using such plant-based raw materials contributes to global sustainability without depletion of scarce resources. Furthermore, bio-based materials may offer the advantages of biodegradability and utility in composting subsequent to their primary use. Among them, natural plant oils, such as soybean, palm, canola, and sunflower oils, are expected as an ideal alternative chemical feedstock, since plant oils are found in abundance in the world. Triglyceride oils have been extensively used for various applications such as coatings, inks, agrochemicals *etc*. [32]. These oil-based polymeric materials, however, do not show properties of rigidity and strength required for structural applications by themselves. In some cases, therefore, triglyceride was a minor component in polymeric materials; this is used solely as a modifier to improve their physical properties.

Epoxidized plant oils are commercially available as stabilizers for the processing of poly(vinyl chloride) and modifiers for coatings [33,34]. Acrylates and polyols derived from epoxidized plant oils have also been used as a monomer for preparation of bio-based polymeric materials. Furthermore, various cationic polymerization of epoxidized plant oils can be achieved by photoinitiators, latent catalysts, or acid catalysts. These epoxy compounds from renewable resources possess high potential as a starting material for bio-based thermosetting plastics [35–38]. The composites of plant oil-based

network polymers from epoxidized plant oils and inorganic substances were developed [39–41]. The acid-catalyzed curing of epoxidized plant oils in the presence of an organophilic montmorillonite produced the triglyceride-clay composites with homogeneous structure, in which silicate layers of the clay were intercalated and randomly distributed in the polymer matrix. The barrier property of the plant oil-based network polymer toward water vapor was remarkably improved by the incorporation of the organophilic clay. The curing of epoxidized plant oils with 3-glycidoxypropyltrimethoxysilane produced biodegradable nanocomposites, in which both oxirane groups of epoxidized plant oil and 3-glycidoxypropyltrimethoxysilane were copolymerized to produce an organic polymer matrix, simultaneously forming silica network.

This study deals with synthesis of new green nanocomposites from epoxidized plant oils and oxirane-containing POSS derivatives. The introduction of the oxirane-containing POSS is anticipated an uniform distribution in the polymer matrix by the copolymerization of epoxidized plant oils and POSS derivatives, and an improvement of coating and mechanical properties of plant oil-based network polymer. In this study, three POSS derivatives were used for preparation of green nanocomposites (Figure 1).

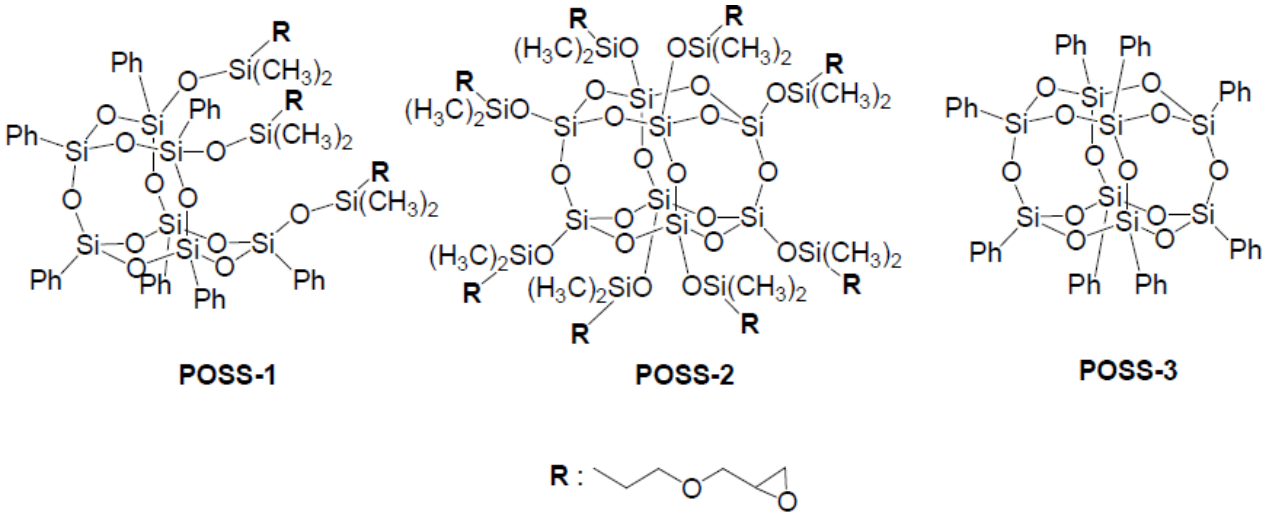

Figure 1. Structure of POSS used in this study.

2. Experimental Section

2.1. Materials

Epoxidized soybean and linseed oils (ESO and ELO) were gifts from Kao Co. (Tokyo, Japan) and Daicel Co. (Osaka, Japan), respectively. A thermally-latent cationic catalyst (benzylsulfonium hexafluoroantimonate derivative, Sun-Aid SI-60L) was provided by Sanshin Chemical Industry Co. (Yamaguchi, Japan) Tris(glycidoxypropyl)dimethylsiloxyphenylsilsesquioxane (POSS-1), octakis(glycidoxypropyl) dimethylsiloxyphenylsilsesquioxane (POSS-2), and octaphenylsilsesquioxane (POSS-3) were provided by JNC Petrochemical Co. (Tokyo, Japan).

2.2. Synthesis of Green Nanocomposites

The following procedure was typically used in the synthesis of green nanocomposites. A mixture of ESO (1.8 g) and POSS-1 (0.2 g) was dissolved in 3 mL of chloroform, and a thermally-latent cationic catalyst (20 μL) was added to the solution. The solution was coated by using a film applicator with slit thickness of 50 μm on a glass plate, and then the solvent was allowed to evaporate at room temperature. The residual mixture was kept at 140 ℃ for 2 h to give ESO/POSS-1 nanocomposite (90:10 wt%). For evaluation of mechanical properties, a test piece of 1 mm width was prepared in a Teflon mold (17 mm × 40 mm × 1 mm) under the same conditions. Other composites were synthesized by a similar procedure.

2.3. Measurements

^{1}H nuclear magnetic resonance (NMR) spectrum was recorded on a Bruker DPX-400 instrument (Bruker Co., Billerica, MA, USA). Epoxidized plant oil was dissolved with chloroform-d, and the solution was measured with tetramethylsilane as an internal reference. Fourier-transform infrared spectroscopy (FT-IR) was measured at room temperature by a Spectrum One (Perkin-Elmer Inc., Waltham, MA, USA). In all cases, 16 scans were used to record the spectra. Transmission electron microscopy (TEM) and electron probe X-ray microanalysis (EPMA) image were obtained by using a JEM-1220 (JEOL Ltd., Tokyo, Japan) at an accelerating voltage of 100 kV and a Horiba E-MAX 7000 (Horiba, Ltd, Kyoto, Japan) at accelerating voltage of 10 kV, respectively. Film properties were evaluated by a Fischerscope H100VS microhardness tester (Fischer Technology Inc., Sindelfingen, Germany) with a test force of 40 mN. The total work and elastic deformation volumes were calculated by the area of the compression curves of the loading and unloading process. Gloss value of the films was measured at 60 °by a Horiba IG-330 gloss checker (Horiba, Ltd, Kyoto, Japan). Dynamic mechanical analysis (DMA) was carried out by using an Exstar 6000 (Hitachi High-Tech Science Co., Tokyo, Japan) with frequency of 1 Hz at a heating rate of 3 ℃·min^{-1}. Tensile properties were measured by a RTM-500 (Orientec Co., Tokyo, Japan).

3. Results and Discussion

3.1. Synthesis of Green Nanocomposites

In this study, epoxidized soybean and linseed oils (ESO and ELO) were used as monomers for organic matrices. The oxirane group numbers of ESO and ELO per molecule, determined by ^{1}H-NMR, were 3.4 and 5.5, respectively. A mixture of the epoxidized plant oil, POSS, and thermally-latent cationic catalyst was coated on a glass slide, followed by the curing at 140 ℃ for 2 h to produce green nanocomposites with high transparency. The resulting nanocomposites were insoluble for common organic solvents and water. During the reaction, the oxirane groups of epoxidized plant oil and POSS reacted with each other to form the network structure.

In the FT-IR spectrum of the green nanocomposite, a characteristic peak at ca. 820 cm^{-1}, ascribed to the C-C antisymmetric stretch of the oxirane groups of epoxidized plant oil and POSS, was not observed,

and a broad peak centered at 3400 cm^{-1} arising from the O-H stretch appeared (Figure 2). These data indicate the consumption of oxirane groups and the formation of hydroxyl-terminated network structure.

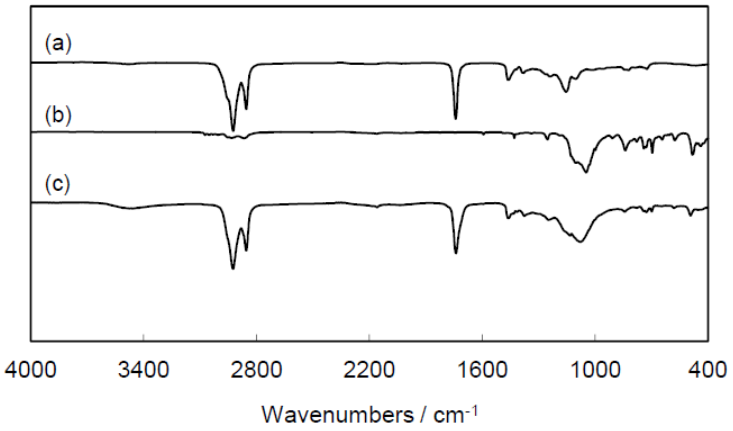

Figure 2. FT-IR spectra of (**a**) ESO; (**b**) POSS-1; and (**c**) ESO/POSS-1 nanocomposite (90:10 wt%).

3.2. Nanostructural Analysis of Green Nanocomposites

The nanostructure of ESO/POSS-1 nanocomposite was observed by TEM and electron probe X-ray microanalysis (EPMA) (Figure 3). The theoretical size of POSS compounds is 1–3 nm. If a few cubes form clusters, their sizes easily reach 10–20 nm. In the TEM image of the ESO/POSS-1 nanocomposite, some small clusters were observed and the cohesions were dispersed in the plant oil-based organic matrix. The EPMA image showed uniform dispersion of inorganic particles in nanometer-size. These data indicate the formation of homogeneous structure of the nanocomposites. On the other hand, the ESO/POSS-3 (95:5 wt%) composite, in which the organic polymer and POSS were not linked via covalent bonds was opaque. This is because of the aggregation of POSS components in millimeter-size. Furthermore, the ESO/POSS-3 composite with 10 wt% of POSS-3 was not obtained due to the aggregation. There were in contrast with the TEM and EPMA images of the ESO/POSS-1 nanocomposite. These data strongly suggest that the covalent bonds between the organic and inorganic units suppress the aggregation of POSS and are required for the plant oil-based nanocomposites.

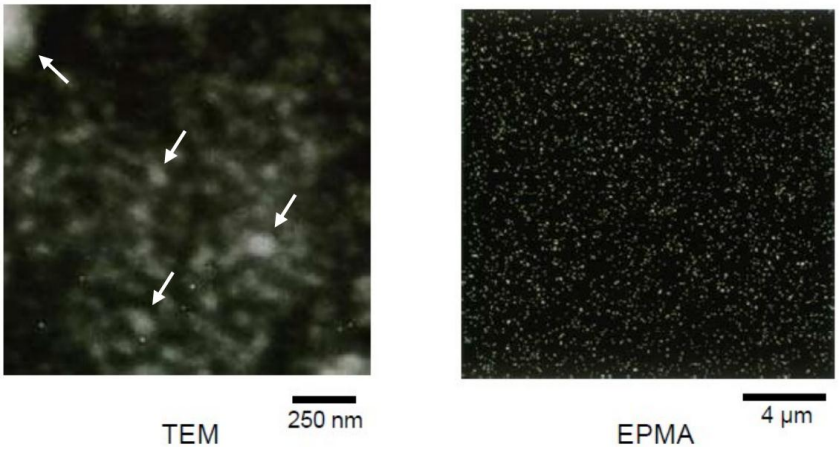

Figure 3. TEM and EPMA images of ESO/POSS-1 nanocomposite (90:10 wt%).

3.3. Film Properties of Green Nanocomposites

The film properties of the green nanocomposites from epoxidized plant oil and oxirane-containing POSS (POSS-1 and POSS-2) were investigated and were summarized in Table 1. The ESO homopolymer was a soft film with pencil scratch hardness of 2B, and the surface was tacky. On the other hand, the transparent films with glossy surfaces were obtained by the addition of 10 wt% POSS-1 or POSS-2. The gloss values of the ESO-based nanocomposites at 60 ° were 113 (POSS-1) and 114 (POSS-2), respectively. The pencil scratch hardness, universal hardness, and Young's modulus of the ESO-based nanocomposites were superior to those of the ESO homopolymer, indicating efficient reinforcement by the introduction of POSS units. The epoxy value of POSS-2 is lower than that of ESO and POSS-1. The hardness and Young's modulus of the ESO/POSS-2 nanocomposite were larger than those of the ESO/POSS-1 nanocomposite, which might be because of the higher content of the reactive oxirane groups of POSS-2. We also measured W_e/W_{tot} of the films (W_e: work volume of elastic deformation; W_{tot}: total work volume), which could be regarded as elasticity. The value of the nanocomposites was slightly lower than that of the ESO homopolymer, probably due to the introduction of the inorganic components.

Table 1. Film properties of green nanocomposites.

Entry	Epoxidized Plant Oil	POSS [a]	Pencil Scratch Hardness	Universal Hardness [b]/N mm^{-2}	Young's Modulus [b]/MPa	W_e/W_{tot} [b,c]/%
1	ESO	-[d]	2B	9	210	90
2	ESO	1 (10)	2H	16	450	78
3	ESO	2 (10)	4H	23	700	68
4	ELO	-[d]	2H	47	1190	45
5	ELO	1 (10)	5H	49	1620	39
6	ELO	2 (10)	> 6H	55	1760	42

[a] In parenthesis: amount of POSS (wt%); [b] Determined by microhardness tester; [c] W_e: work volume of elastic deformation; W_{tot}: total work volume; [d] No additive.

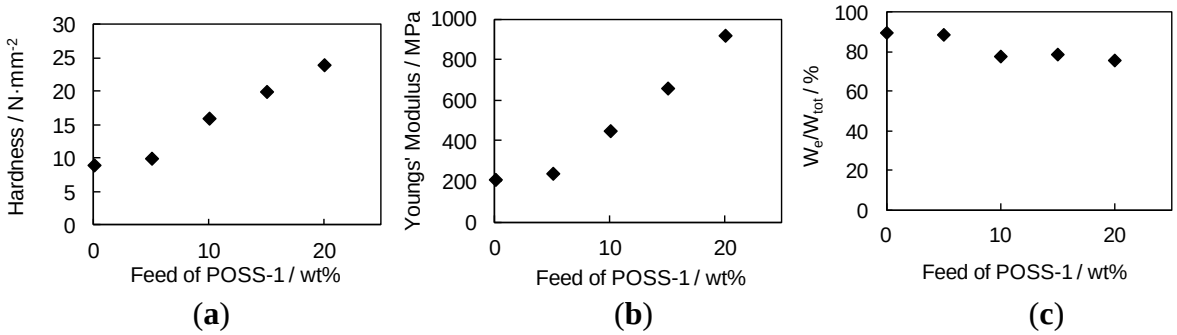

Figure 4. Relationships between feed ratio of POSS-1 and film properties of ESO/POSS-1 nanocomposite; (**a**) hardness; (**b**) Young's modulus; and (**c**) W_e/W_{tot}.

Figure 4 shows relationships between the feed ratio of POSS-1 and film properties of the ESO-based nanocomposite coatings. The universal hardness and Young's modulus of the nanocomposite increased, and W_e/W_{tot} slightly decreased as a function of the feed ratio of POSS-1. The ELO/POSS nanocomposites were prepared by similar procedures. By the addition of POSS units, the hardness and Young's modulus

of the nanocomposites were also improved in comparison with those of the ELO homopolymer. The ELO-based nanocomposites showed harder coating properties than the ESO-based nanocomposites. This is due to the higher content of the reactive oxirane groups in ELO, resulting in the higher crosslinking density of the polymer matrix.

3.4. Thermal and Mechanical Properties of Green Nanocomposites

In order to evaluate reinforcement effects of the introduction of POSS units, DMA as a function of temperature was preformed. The storage modulus (E') and loss factor (tanδ) of the ESO homopolymer and the ESO/POSS-1 nanocomposite (90:10 wt%) are shown in Figure 5. A peak attributed to the glass transition, and an absence of a secondary tan δ peak were observed for the nanocomposite, supporting the homogeneous structure of the nanocomposite. The glass transition temperature (T_g) of the nanocomposite (9 ℃) was higher than that of the ESO homopolymer (−10 ℃). At higher temperature, E' of the nanocomposite was larger than that of the ESO homopolymer, which is due to the reinforcement by the introduction of the inorganic components. Above T_g, E' of the nanocomposite was almost constant, indicating the quantitative consumption of the oxirane groups, which was also confirmed by FT-IR (Figure 2).

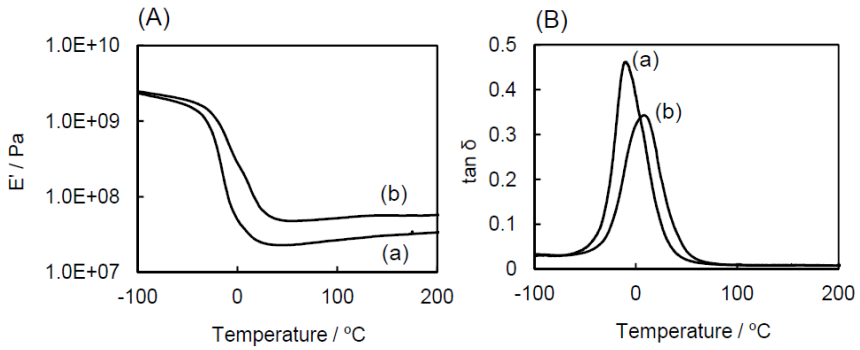

Figure 5. Dynamic viscoelasticity of (**a**) ESO homopolymer and (**b**) ESO/POSS-1 nanocomposite: (**A**) storage modulus (E'); (**B**) loss factor (tanδ).

Table 2. Mechanical properties of green nanocomposites.

Entry	Epoxidized Plant Oil	POSS [a]	T_g [b]/℃	E'+ 100 ℃ [b]/× 10^7 Pa	Crosslinking density [b]/× 10^{-3} mol m^{-3}	Tensile Modulus [c]/MPa	Maximum Stress [c]/MPa	Strain at Break [c]/%
1	ESO	- [d]	−10	3.1	3.15	13	1.0	9
2	ESO	**1** (10)	8	5.6	5.48	18	2.5	20
3	ESO	**2** (10)	9	5.7	5.96	15	2.7	17
4	ESO	**3** (5)	−7	3.4	3.43	14	1.1	10
5	ELO	- [d]	48	9.1	9.97	240	15.7	6
6	ELO	**1** (10)	55	12.0	13.3	260	16.9	11
7	ELO	**2** (10)	54	14.2	15.6	280	18.1	9

[a] In parenthesis: amount of POSS (wt%); [b] Determined by DMA; [c] Determined by tensile rest; [d] No additive.

Table 2 summarizes the results of DMA and tensile test of the nanocomposites. The increase of T_g was observed for all the nanocomposites of POSS-1 and POSS-2. In case of the ESO/POSS-3 composite, such increase was not found. This is because of the structural difference of the nanocomposites at the

nanometer scale. These results suggest that the nanoarchitecture manipulation is clearly related to improvement of the bulk properties of the hybrid materials.

The crosslinking density (ρ) was determined by using kinetic theory of rubber elasticity as follows [42];

$$\rho = E'/3\varphi RT \quad (1)$$

where E' is storage modulus at peak temperature of tan δ + 40 °C, φ is a front factor (assumed as φ = 1), R is gas constant, and T is absolute temperature. The crosslinking density of the nanocomposites was larger than that of the corresponding plant oil-based homopolymers. Such increase of the crosslinking density was not observed in the ESO/POSS-3 composite. The introduction of POSS units into plant oil-based polymer network via covalent bonds restricted the segmental motion of the polymer chain and the covalent bond between the plant oil-based polymer and POSS units prevented the aggregation of POSS units. As a result, POSS units were well-dispersed in the organic matrix for the ESO/POSS-1 and ESO/POSS-2 nanocomposites.

Figure 6 shows strain-stress curves of the ESO homopolymer and the ESO/POSS-1 nanocomposite. For ESO/POSS-1 nanocomposite, the maximum tensile stress was much improved, whereas the tensile modulus of the nanocomposite was only slightly larger than that of the ESO homopolymer. The elongation at break of the nanocomposite was larger than that of the ESO homopolymer. Similar behaviors were observed in the ESO/POSS-2 and ELO-based nanocomposites (Table 2). On the other hand, such improvements in the mechanical properties were not found in the ESO/POSS-3 composite, suggesting that nanoarchitecture manipulation strongly affected the mechanical properties. The tensile modulus and maximum stress of the ELO-based nanocomposites were enormously larger than those of the ESO-based nanocomposites, which is due to higher crosslinking density of the ELO polymer matrix. These data are in good accordance with those of the film properties (Table 1).

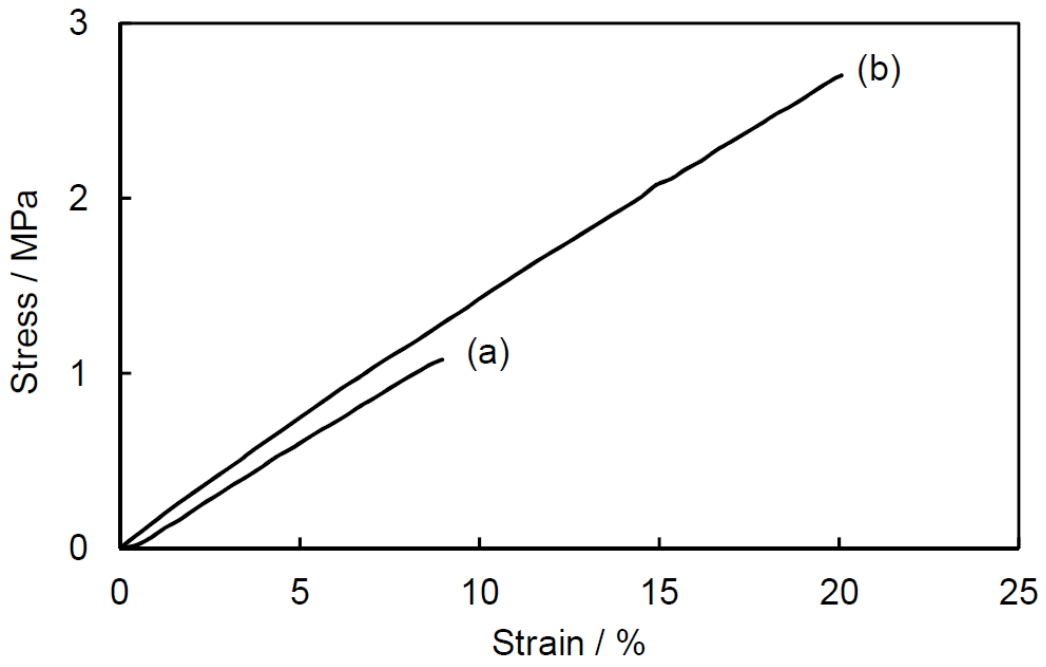

Figure 6. Strain-stress curves of (**a**) ESO homopolymer and (**b**) ESO/POSS-1 nanocomposite (90:10 wt%).

4. Conclusions

In this study, green nanocomposites based on renewable plant oils and POSS have been developed. The acid-catalyzed curing of epoxidized plant oil and the oxirane-containing POSS produced the transparent nanocomposites, in which the organic and inorganic components were linked by covalent bonds. The TEM and EPMA images revealed the homogeneous structure of the nanocomposites at micrometer scale. The incorporation of POSS units greatly enhanced the coating and mechanical properties of the nanocomposites. The present study clearly showed that the nanoarchitecture manipulation offered improvement of the bulk properties of the composite materials.

Acknowledgments

The authors would like to thank JNC Petrochemical Corporation for measuring the nanostructural analysis. This study supported by a Grant-in-Aid for Young Scientists from Japan Society for the Promotion of Science (JSPS).

Author Contributions

Hiroshi Uyama and Shiro Kobayashi designed the experiments; Takashi Tsujimoto performed the experiments and analyzed the data; Hisao Oikawa and Mikio Yamahiro contributed POSSs and performed Nanostructural analyses; the paper was written by Takashi Tsujimoto.

Conflicts of Interest

The authors declare no conflict of interest.

References

1. Sanchez, C.; Soler-Illia, G.J.A.A.; Ribot, F.; Lalot, T.; Mayer, C.R.; Cabuil, V. Designed hybrid organic-inorganic nanocomposites from functional nanobuilding blocks. *Chem. Mater.* **2001**, *13*, 3061–3083.
2. Spange, S.; Grund, S. Nanostructured organic-inorganic composite materials by twin polymerization of hybrid monomers. *Adv. Mater.* **2009**, *21*, 2111–2116.
3. Guan, Y.; Zhang, B.; Tan, X.; Qi, X.; Bian, J.; Peng, F.; Sun, R. Organic-inorganic composite films based on modified hemicelluloses with clay nanoplatelets. *ACS Sustain. Chem. Eng*. **2014**, *2*, 1811–1818.
4. Hensbergen, J.A.; Liu, M.; Burford, R.P.; Lowe, A.B. Simultaneous ROMP and titania sol-gel reactions and nanodispersed functional organic-inorganic composite hybrid materials. *J. Mater. Chem. C* **2015**, *3*, 693–702.
5. Cordes, D.B.; Lickiss, P.D.; Rataboul, F. Recent developments in the chemistry of cubic polyhedral oligosilsesquioxanes. *Chem. Rev.* **1996**, *110*, 2081–2173.
6. Murugavel, R.; Voigt, A.; Walawalkar, M.G.; Roesky, H.W. Hetero- and metallasiloxanes derived from silanediols, disilanols, silanetriols, and trisilanols. *Chem. Rev.* **1996**, *96*, 2205–2236.

7. Laine, R.M. Nanobuilding blocks based on the $[OSiO_{1.5}]_x$ (x = 6, 8, 10) octasilsesquioxanes. *J. Mater. Chem.* **2005**, *15*, 3725–3744.
8. Zeng, J.; Kumer, S.; lyer, S.; Schiraldi, D.A.; Gonzalez, R.I. Reinforcement of poly(ethylene terephthalate) fibers with polyhedral oligomeric silsesquioxanes (POSS). *High Perform. Polym.* **2005**, *17*, 403–424.
9. Lickiss, P.D.; Rataboul, F. Fully condensed polyhedral oligosilsesquioxanes (POSS): From synthesis to application. *Adv. Org. Chem.* **2008**, *57*, 1–116
10. Wu, J.; Haddad, T.S.; Mather, P.T. Vertex group effects in entangled polystyrene-polyhedral oligosilsesquioxane (POSS) copolymers. *Macromolecules* **2009**, *42*, 1142–1152.
11. Kodal, M.; Sirin, H.; Ozkoc, G. Effects of reactive and nonreactive POSS types on the mechanical, thermal, and morphological properties of plasticized poly(lactic acid). *Polym. Eng. Sci.* **2014**, *54*, 264–275.
12. Zhao, Y.; Schiraldi, D.A. Thermal and mechanical properties of polyhedral oligomeric silsesquioxane (POSS)/polycarbonate composites. *Polymer* **2005**, *46*, 11640–11647.
13. Castañeda, L.; López-Suárez, A.; Tiburcio-Silver, A. The role of polyhedral oligomeric silsesquioxane on the thermo-mechanical properties of polyoxymethylene copolymer based nanocomposites. *J. Nanosci. Nanotechnol.* **2010**, *10*, 1349–1360.
14. Kuo, S.W.; Chang, F.C. POSS related polymer nanocomposites. *Prog. Polym. Sci.* **2011**, *36*, 1649–1696.
15. Choi, J.; Yee, A.F.; Laine, R.M. Toughening of cubic silsesquioxane epoxy nanocomposites using core-shell rubber particles: A three-component hybrid system. *Macromolecules* **2004**, *37*, 3267–3276.
16. Lligadas, G.; Ronda, J.C.; Galià, M.; Cádiz, V. Bionanocomposites from renewable resources: Epoxidized linseed oil-polyhedral oligomeric silsesquioxanes hybrid. *Biomacromolecules* **2006**, *7*, 3521–3526.
17. Xiao, F.; Sun, Y.; Xiu, Y.; Wong, C.P. Preparation, thermal and mechanical properties of POSS epoxy hybrid composites. *J. Appl. Polym. Sci.* **2007**, *104*, 2113–2121.
18. Wahab M.A.; Mya, K.Y.; He, C. Synthesis, morphology, and properties of hydroxyl terminated-POSS/polyimide low-k nanocomposite films. *J. Polym. Sci. A. Polym. Chem.* **2008**, *46*, 5887–5896.
19. Tanaka, K.; Adachi, S.; Chujo, Y. Structure-property relationship of octa-substituted POSS in thermal and mechanical reinforcements of conventional polymers. *J. Polym. Sci. A Polym. Chem.* **2009**, *47*, 5690–5697.
20. Escudé, N.C.; Chen, E.Y.X. Stereoregular methacrylate-POSS hybrid polymers: Syntheses and nanostructured assemblies. *Chem. Mater.* **2009**, *21*, 5743–5753.
21. Ahn, B.; Hirai, T.; Jin, S.; Rho, Y.; Kim, K.W.; Kakimoto, M.; Gopalan, P.; Hayakawa, T.; Ree, M. Hierarchical structure in nanoscale thin films of a poly(styrene-*b*-methacrylate grafted with POSS) (PS_{214}-*b*-$PMAPOSS_{27}$). *Macromolecules* **2010**, *43*, 10568–10581.
22. Matějka, L.; Murias, P.; Pleštil, J. Effect of POSS on thermomechanical properties of epoxy-POSS nanocomposites. *Eur. Polym. J.* **2012**, *48*, 260–274.

23. Lin, H.; Qu, J.; Zhang, Z.; Dong, J.; Zou, H. Ring-opening polymerization reaction of polyhedral oligomeric silsesquioxanes (POSSs) for preparation of well-controlled 3D skeletal hybrid monoliths. *Chem. Commun.* **2013**, *49*, 231–233.
24. Szarc-Rzepka, K.; Marciniec, B.; Jesionowski, T. Immobilization of multifunctional silsesquioxane cage on precipitated silica supports. *Adsorption* **2013**, *19*, 483–494.
25. Oleksy, M.; Szwarc-Rzepka, K.; Heneczkowski, M.; Oliwa, R.; Jesionowski, T. Epoxy resin composite based on functional hybrid fillers. *Materials* **2014**, *7*, 6064–6091.
26. Wysokowski, M.; Materna, K.; Walter, J.; Petrenko, I.; Stelling, A.L.; Bazhenov, V.V.; Klapiszewski, L.; Szatkowski, T.; Lewandowska, O.; Stawski, D.; *et al*. Solvothermal synthesis of hydrophobic chitin-polyhedral oligomeric silsesquioxane (POSS) nanocomposites. *Int. J. Biol. Macromol.* **2015**, *78*, 224–229.
27. Ogi, K.; Miyauchi, S.; Naka, K. Amphiphilic POSS-core dendrons for optically transparent thermoplastic films with tunable wettability. *Polym. J.* **2015**, *47*, 259–266.
28. Lee, A.; Lichtenhan, J.D. Viscoelastic responses of polyhedral oligosilsesquioxane reinforced epoxy systems. *Macromolecules* **1998**, *31*, 4970–4974.
29. Choi, J.; Harcup, J.; Yee, A.F.; Zhu, Q.; Laine, R.M. Organic/inorganic hybrid composites from cubic silsesquioxanes. *J. Am. Chem. Soc.* **2001**, *123*, 11420–11430.
30. Ni, Y.; Zheng, S.; Nie, K. Morphology and thermal properties of inorganic-organic hybrids involving epoxy resin and polyhedral oligomeric silsesquioxanes. *Polymer* **2004**, *45*, 5557–5568.
31. Nagarajan, V.; Mohanty, A.K.; Misra, M. Sustainable green composites: Value addition to agricultural residues and perennial grasses. *ACS Sustain. Chem. Eng.* **2013**, *1*, 325–333.
32. Biermann, U.; Friedt, W.; Lang, S.; Lühs, W.; Machmüller, G.; Metzger, J.O.; Rüsch gen Klaas, M.; Schäfer, H.J.; Schneider, M.P. New syntheses with oils and fats as renewable raw materials for the chemical industry. *Angew. Chem. Int. Ed.* **2000**, *39*, 2206–2224.
33. Petrović, Z.S.; Zhang, W.; Javni, I. Structure and properties of polyurethenes prepared from triglyceride polyols by ozonolysis. *Biomacromolecules* **2005**, *6*, 713–719.
34. Biresaw, G.; Liu, Z.S.; Erhan, S.Z. Investigation of the surface properties of polymeric soaps obtained by ring-opening polymerization of epoxidized soybean oil. *J. Appl. Polym. Sci.* **2008**, *108*, 1976–1985.
35. Chakrapani, S.; Crivello, J.V. Synthesis and photoinitiated cationic polymerization of epoxidized castor oil and its derivatives. *J. Macromol. Sci. Pure Appl. Chem.* **1998**, *A35*, 1–20.
36. Tran, P.; Graiver, D.; Narayan, R. Biocomposites synthesized from chemically modified soy oil and biofibers. *J. Appl. Polym. Sci.* **2006**, *102*, 69–75.
37. Shibata, M.; Teramoto, N.; Someya, Y.; Suzuki, S. Bio-based nanocomposites composed of photo-cured epoxidized soybean oil and supramolecular hydroxystearic acid nanofibers. *J. Polym. Sci. Part B Polym. Phys.* **2009**, *47*, 669–673.
38. Wang, R.; Schuman, T.P. Vegetable oil-derived epoxy monomers and polymer blends: A comparative study with review. *Express Polym. Lett.* **2013**, *7*, 272–292.
39. Uyama, H.; Kuwabara, M.; Tsujimoto, T.; Nakano, M.; Usuki, A.; Kobayashi, S. Organic-inorganic hybrids from renewable plant oils and clay. *Macromol. Biosci.* **2004**, *4*, 354–360.

40. Miyagawa, H.; Misra, M.; Drazal, L.T.; Mohanty, A.K. Novel biobased nanocomposites from functionalized vegetable oil and organically-modified layered silicate clay. *Polymer* **2005**, *46*, 445–453.
41. Tsujimoto, T.; Uyama, H.; Kobayashi, S. Synthesis of high-performance green nanocomposites from renewable natural oils. *Polym. Degrad. Stable* **2010**, *95*, 1399–1405.
42. Ogata, M.; Kinjyo, N.; Tawata, T. Effect of crosslinking on physical properties of phenol-formaldehyde novolac cured epoxy resins. *J. Appl. Polym. Sci.* **1993**, *48*, 583–601.